Exact solutions of a restricted ballistic deposition model on a one-dimensional staircase

Hyunggyu Park
Department of Physics, Inha University, Inchon 402-751, Korea

Meesoon Ha and In-mook Kim
Department of Physics, Korea University, Seoul 136-701, Korea
(Received 11 October 1994)

The surface structure of a restricted ballistic deposition model is examined on a one-dimensional staircase with free boundary conditions. In this model, particles can be deposited only at the steps of the staircase. We set up recurrence relations for the surface fluctuation width W using the generating function method. Steady-state solutions are obtained exactly given system size L. In the infinite-size limit, W diverges as L^{α} with the scaling exponent $\alpha = \frac{1}{2}$. The dynamic exponent β ($W \sim t^{\beta}$) is also found to be $\frac{1}{2}$ by solving the recurrence relations numerically. This model can be viewed as a simple variant of the model which belongs to the Kardar-Parisi-Zhang (KPZ) universality class ($\alpha_{KPZ} = \frac{1}{2}$, $\beta_{KPZ} = \frac{1}{3}$). Comparing its deposition time scale with that of the single-step model, we argue that β must be the same as $\beta_{KPZ}/(1-\beta_{KPZ})$, which is consistent with our finding.

PACS number(s): 05.40.+j, 68.35.Fx, 68.55.Jk

I. INTRODUCTION

Recently, the dynamics of growing surfaces or interfaces has been one of the most interesting problems in surface science. Crystal growth, dielectric breakdown, fluid displacement in porous media, vapor deposition, spray painting and coating, biological growth, and electrodeposition are only a few examples which are important from both theoretical and practical points of view [1,2]. A stochastically growing surface exhibits nontrivial scaling behavior and evolves to a steady state without any characteristic time or spatial scale. This observation has led to the development of a general scaling approach for describing a growing surface which exhibits a self-affine fractal geometry [3]. In particular, the dynamic scaling approach [4,5] has been applied to the study of a variety of theoretical models of growing surfaces.

The important feature of a growing surface is the roughness of the surface induced by stochastic noise and its roughness can be characterized by few scaling exponents. A fundamental question is how to classify rough surfaces given the dynamic rules of deposition processes. The simplest model is the random deposition model, which has no interactions between neighboring columns. This model can be solved exactly for any system size. It produces a rough surface in which the surface width grows with the square root of time but never reaches a steady state for finite systems. When interactions are introduced between columns, the surface width for finite systems saturates in the long-time limit. The evolution of the surface width W is described by a dynamic scaling relation

$$W = L^{\alpha} f(t/L^{z}), \tag{1}$$

where L is the linear dimension of the system, t is the time, and the scaling function f has the asymptotic behaviors $f(x) \sim x^{\beta}$, with $\beta = \alpha/z$, for $x \ll 1$, and $f(x) \sim$ constant for $x \gg 1$. Consequently, the limiting behaviors of the width are

$$W \sim \begin{cases} L^{\alpha} & (t \gg L^{z}), \\ t^{\beta} & (t \ll L^{z}). \end{cases} \tag{2}$$

Many stochastic models with intercolumnar interactions have been introduced and extensively studied. One simple example is the random deposition model with surface diffusion [6]. A deposited particle diffuses on the surface and is incorporated into the deposit upon reaching a local minimum. This rearrangement process reduces the surface tension of the deposit and the surface becomes relatively smooth with scaling exponents $\alpha \simeq \frac{1}{2}$ and $\beta \simeq \frac{1}{4}$ in $(1+1)$ dimensions. These values are obtained by numerical simulations and the exact solutions are not available as yet. It has been argued that this model can be described by a continuum equation with a noise source,

$$\frac{\partial h}{\partial t} = \nu \nabla^2 h + \eta, \tag{3}$$

where h denotes the deviation of the local height of the deposit from its average value and η is a Gaussian random noise. The solution of Eq. (3) yields $\alpha = 1/2$ and $\beta = 1/4$ in $(1+1)$ dimensions [7], which is consistent with the numerical results. Many other models with different rearrangement rules have been studied by numerical simulations and also by solving the corresponding continuum equations. However, both methods have their own weak points. Numerical simulations often do not reach the scaling regime within a reasonable amount of time. A continuum equation corresponding to a given stochastic model may be reasonably guessed but it is very difficult

to prove that it correctly describes the stochastic model. For example, there has been a great deal of controversies over which continuum equation describes the Wolf-Villain model [8]. It is important to find exact solutions for stochastic models but it is usually formidable.

Some other stochastic models, like the ballistic deposition model [5,9], the single-step model [5,10,11], and the restricted solid-on-solid model [12], behave differently from the particle-rearrangement models. Numerical simulations on these models provide the scaling exponents $\alpha \simeq \frac{1}{2}$ and $\beta \simeq \frac{1}{3}$ in $(1+1)$ dimensions. In these models, the lateral current of particles along the surface is not conserved, so evolution of the surface involves lateral growth. It has been argued that all these models can be described by the Kardar-Parisi-Zhang (KPZ) equation [13]

$$\frac{\partial h}{\partial t} = \nu \nabla^2 h + \frac{\lambda}{2}(\nabla h)^2 + \eta, \tag{4}$$

where the nonlinear term represents the lateral growth. Dynamic renormalization group calculations [14] for Eq. (4) yield $\alpha = 1/2$ and $\beta = 1/3$ in $(1+1)$ dimensions (KPZ universality class), which is consistent with the numerical results. However, higher-dimensional cases are not settled yet.

In this paper, we present a nontrivial stochastic model which can be solved exactly for finite system sizes in $(1+1)$ dimensions. This model is similar to the ballistic deposition model, but height differences between neighboring columns are restricted to be positive or zero: $h_{i+1} - h_i \geq 0$, where h_i is the column height at site i. The resulting surface should look like a one-dimensional ascending staircase with variable widths of terraces and variable heights of steps (see Fig. 1). Particles can be deposited only at the steps of the staircase, otherwise dynamic processes are rejected. From the master equation of this model with open boundary conditions, we set up recurrence relations for the surface fluctuation width W using the generating function method. In the steady-state limit, we are able to extract the exact solutions for system size L from which we obtain $\alpha = \frac{1}{2}$ in the infinite-size limit. We also find $\beta = \frac{1}{2}$ by solving the recurrence relations numerically. No statistical errors are involved in this estimate because the ensemble average has already been done in the recurrence relations. It is somewhat surprising at first glance because this model can be viewed as a simple variant of the single-step model (KPZ universality class) [5,11] by rotating the surface clockwise by 45°, but the values of the exponents are different from those of the single-step model. We argue that the dynamic exponent β must be the same as $\beta_{KPZ}/(1-\beta_{KPZ})$ by comparing its deposition time scale with that of the single-step model, which is consistent with our finding. Considering this argument the other way around, one can say that our results for these scaling exponents are the best estimates for stochastic models in the KPZ universality class.

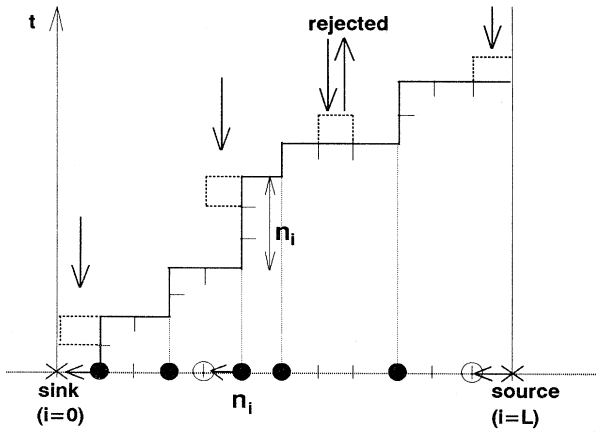

FIG. 1. Dynamic processes of the RBD model. Deposition of particles can occur only at the steps of the surface. The corresponding particle dynamics model is also shown.

The outline of this paper is as follows. In Sec. II, we describe our model and discuss its relation to a particle dynamics model, a spin-exchange model, and the single-step model. In Sec. III, we define the generating function and set up the recurrence relations. In Sec. IV, we find the exact solutions in the steady-state limit and present the numerical estimate for β. Comparison with the single-step model is given in Sec. V and we conclude in Sec. VI with a brief summary.

II. RESTRICTED BALLISTIC DEPOSITION MODEL

Consider the ballistic deposition (BD) model [5] in $(1+1)$ dimensions. In the BD model, a particle falls down along a straight line and sticks to the surface of the deposit. We introduce a restricted ballistic deposition (RBD) model by allowing only deposition processes which preserve the morphology of an ascending staircase of the surface, i.e.,

$$n_i(t) \equiv h_{i+1}(t) - h_i(t) \geq 0 \qquad \text{for all} \quad i, \tag{5}$$

where $h_i(t)$ is the column height of site i at time t and $n_i(t)$ is the height of the step between ith and $(i+1)$th sites.

We start with a surface of horizontal length L with unit step heights at every possible step, i.e., $n_i(0) = 1$ for $i = 1, 2, \ldots, L-1$, or equivalently $h_i(0) = i$ for $i = 1, \ldots, L$. (The reason why we take this particular configuration as an initial state will be discussed in Sec. IV.) First, select a site i randomly and drop a particle along a straight line. The particle becomes part of the deposit when it contacts a particle in the deposit only if the resulting step heights are all positive or zero [Eq. (5)]. Otherwise, the particle is rejected (see Fig. 1). When a site i $(\neq 1, L)$ is chosen at time t, the deposition process can occur for $n_i(t) > 0$ and the rejection process for $n_i(t) = 0$. Then n_i and n_{i-1} are updated as

$$\begin{aligned} n_i(t+\Delta t) &= 0, \\ n_{i-1}(t+\Delta t) &= n_{i-1}(t) + n_i(t), \end{aligned} \tag{6}$$

where Δt is the time elapsed during one deposition at-

tempt. Notice that Eq. (6) is valid for both deposition and rejection processes. This is the key point of obtaining rather simple recurrence relations to be solved exactly.

We use *free* boundary conditions. When a site $i = 1$ is chosen, the deposition and rejection processes can be described by the first equation of Eq. (6). At site L, only the deposition process can occur (no rejection) such that

$$n_{L-1}(t + \Delta t) = n_{L-1} + 1. \tag{7}$$

This equation can be identified as the second equation of Eq. (6) by defining $n_L \equiv 1$. (This is useful to write simple recurrence relations in Sec. III.)

The RBD model can be mapped on a one-dimensional particle dynamics model with directed diffusion and mass-conserving coalescence processes. The dynamic variable n_i represents the mass of the particle at site i. Equation (6) implies that a particle of mass $n_i(t)$ at site i diffuses to the left and stays there if $n_{i-1}(t) = 0$ (no particle at site $i - 1$ at time t) or coalesces with a particle of mass $n_{i-1}(t)$ at site $i - 1$ if $n_{i-1}(t) > 0$. At the boundaries, there are the input (source) and output (sink) of particles. Particles of unit mass come into the system from the right side of site $L - 1$ and particles of arbitrary mass leave the system to the left side of site 1 as shown in Fig. 1.

One can map this RBD model onto a variant of spin-exchange models, in the same way as the Toom model [15,16] in the low-noise limit is mapped onto one of the spin-exchange models. Details of this mapping can be found in Ref. [16]. Our model does not belong to the class of general $\mathcal{M}^{(k)}$ spin-exchange models (see Appendix A of [16]). This aspect will be discussed further elsewhere.

One can find a close resemblance between the RBD model and the single-step model if not *sticky* particles but *smooth* particles are used in the RBD model. Now a particle falls down along a straight line and becomes part of the deposit when it hits the ground. Of course, the surface of the RBD model is rotated by 45° from the surface of the single-step model. Both models restrict deposition only at the steps (or valleys on the 45°-rotated surface; see Fig. 2). Unfortunately our model with smooth particles does not yield simple recurrence relations, in contrast to the RBD model with sticky particles. The dynamics with smooth particles cannot be represented by simple equations like Eq. (6) but by equations with conditional statements. However, we argue in Sec. V that these two models exhibit essentially the same scaling behavior if the time-scale difference is taken into account.

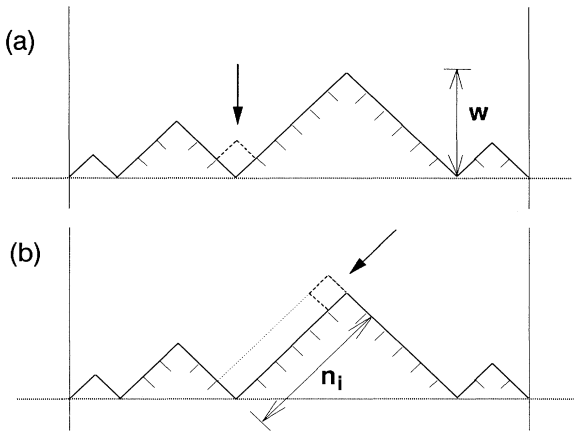

FIG. 2. Deposition processes of (a) the single-step model and (b) the RBD model on the 45°-rotated surface.

III. GENERATING FUNCTION AND RECURRENCE RELATIONS

In this section, we write the master equation for the evolution of the surface in the RBD model with general *inhomogeneous* deposition rates. The deposition rates are parametrized by $\{\kappa_1, \kappa_2, \ldots, \kappa_L\}$ where κ_i is a relative deposition rate at site i with normalization $\sum_i \kappa_i = 1$. The RBD model with ordinary homogeneous deposition rates is restored when all κ_i's are replaced by $1/L$. A surface configuration can be characterized by a state vector $\mathbf{n} = (n_1, n_2, \ldots, n_{L-1})$ if we are not concerned about the overall average height but are interested in relative heights only. We define $P_t(\mathbf{n})$ as the probability to find a configuration $\mathbf{n}$ at time t. Then the master equation can be written as

$$\begin{aligned} P_{t+\Delta t}(\mathbf{n}) = {} & \kappa_1 \delta_{n_1,0} \sum_{m=1}^{\infty} P_t(m, n_2, \ldots) + \kappa_L \theta(n_{L-1}) P_t(n_1, \ldots, n_{L-1} - 1) \\ & + \sum_{i=2}^{L-1} \kappa_i \theta(n_{i-1}) \delta_{n_i,0} \sum_{m=1}^{n_{i-1}} P_t(\ldots, n_{i-2}, n_{i-1} - m, m, n_{i+1}, \ldots) + \sum_{i=1}^{L-1} \kappa_i \delta_{n_i,0} P_t(\mathbf{n}), \end{aligned} \tag{8}$$

where δ is a Kronecker delta function and $\theta(x) = 1$ for $x \geq 1$ and zero otherwise. The first three terms in the right hand side of the above equation describe the deposition processes at the boundaries and inside the boundaries. The last term describes the rejection processes.

Consider the generating function defined as

$$G_t(z_1, z_2, \ldots, z_{L-1}) \equiv \sum_{n_i \geq 0} z_1^{n_1} z_2^{n_2} \cdots z_{L-1}^{n_{L-1}} P_t(\mathbf{n}). \tag{9}$$

Using Eq. (8), one can obtain the generating function at time $t + \Delta t$ in terms of G_t,

$$G_{t+\Delta t}(z_1,\ldots,z_{L-1}) = \kappa_1 G_t(1,z_2,\ldots) + \kappa_L z_{L-1} G_t(z_1,\ldots,z_{L-1}) + \sum_{i=2}^{L-1} \kappa_i G_i(\ldots,z_{i-1},z_{i-1},z_{i+1},\ldots). \quad (10)$$

The ensemble averages of step heights (particle masses) and two-point (mass-mass) correlation functions are obtained by differentiating the generating function and setting all z_i's to be 1 as

$$\langle n_i\rangle_t = \left.\frac{\partial G_t}{\partial z_i}\right|_{\{z\}=1},$$
$$\langle n_i n_j\rangle_t = \left.\frac{\partial}{\partial z_i}\left(z_j\frac{\partial G_t}{\partial z_j}\right)\right|_{\{z\}=1}. \quad (11)$$

Thus the dynamics of the step heights (masses) and two-point correlation functions are given as

$$\begin{aligned}
\langle n_i\rangle_{t+\Delta t} &= (1-\kappa_i)\langle n_i\rangle_t + \kappa_{i+1}\langle n_{i+1}\rangle_t,\\
\langle n_i^2\rangle_{t+\Delta t} &= (1-\kappa_i)\langle n_i^2\rangle_t + 2\kappa_{i+1}\langle n_i n_{i+1}\rangle_t \\
&\quad +\kappa_{i+1}\langle n_{i+1}^2\rangle_t,\\
\langle n_i n_{i+1}\rangle_{t+\Delta t} &= (1-\kappa_i-\kappa_{i+1})\langle n_i n_{i+1}\rangle_t \\
&\quad +\kappa_{i+2}\langle n_i n_{i+2}\rangle_t, \quad (12)\\
\langle n_i n_j\rangle_{t+\Delta t} &= (1-\kappa_i-\kappa_j)\langle n_i n_j\rangle_t + \kappa_{i+1}\langle n_{j+1} n_j\rangle_t \\
&\quad +\kappa_{j+1}\langle n_i n_{j+1}\rangle_t,
\end{aligned}$$

where $i,j = 1,\ldots,L-1$ with $|i-j|\geq 2$ and n_L is set to be 1.

First, we consider the steady state only. The ensemble-averaged masses in the steady state, $\langle n_i\rangle_\infty$, satisfy the recurrence relations

$$\kappa_i\langle n_i\rangle_\infty = \kappa_{i+1}\langle n_{i+1}\rangle_\infty = \cdots = \kappa_L\langle n_L\rangle_\infty = \kappa_L, \quad (13)$$

which leads to

$$\langle n_i\rangle_\infty = \frac{\kappa_L}{\kappa_i}. \quad (14)$$

In the homogeneous case, $\langle n_i\rangle_\infty = 1$ at any site i, so the ensemble-averaged surface looks like an ascending *regular* staircase with unit step heights and unit terrace widths in the steady-state (long-time) limit.

We also find recurrence relations for two-point correlation functions in the steady state as

$$\begin{aligned}
Q_{iL} &= Q_{i+1,L},\\
Q_{ii} &= w_i Q_{i,i+1} + Q_{i+1,i+1},\\
Q_{i,i+1} &= u_{i,i+1} Q_{i,i+2}, \quad (15)\\
Q_{ij} &= u_{ij} Q_{i+1,j} + v_{ij} Q_{i,j+1},
\end{aligned}$$

where Q_{ij}, u_{ij}, v_{ij}, and w_i are defined as

$$Q_{ij} \equiv \kappa_i\langle n_i n_j\rangle_\infty, \quad (16)$$

$$u_{ij} \equiv \frac{1}{1+\kappa_j/\kappa_i}, \qquad v_{ij} \equiv u_{ij}\frac{\kappa_{j+1}}{\kappa_i},$$

and

$$w_i \equiv 2\frac{\kappa_{i+1}}{\kappa_i}, \quad (17)$$

with $Q_{ji} = \frac{\kappa_j}{\kappa_i}Q_{ij}$. It is easy to solve the above recurrence relations numerically for finite values of L. Start from the known value of $Q_{LL} = \kappa_L$. Using the recurrence relations repeatedly, one can find the values of $Q_{L-1,L}$, then $Q_{L-2,L}$ and $Q_{L-1,L-1}$, then $Q_{L-3,L}$ and $Q_{L-2,L-1}$, and so on. Q_{ij} is determined by $Q_{i'j'}$'s only for $i'+j' > i+j$. This brings out an idea of mapping these recurrence relations to a directed random walk problem.

Consider the upper diagonal half of an $L\times L$ square lattice (Fig. 3). We assign appropriate weights, u_{ij}, v_{ij}, w_i, 1, or 0, on the bonds connecting neighboring sites. Now imagine that a walker starts from a lattice site (L,L) and moves only left or down (directed random walk). There are numerous paths along which the walker can reach a site (i,j). A typical path is drawn in Fig. 3. Paths going through the lower diagonal half of the square lattice are excluded. The weight to a path is given as the product of bond weights along the path. Then Q_{ij} can be calculated by summing up path weights for all possible paths. So the formal solutions for Q_{ij} are given as

$$Q_{ij} = Q_{LL}\sum_{\substack{\text{all}\\ \text{possible paths}}}\prod_{\text{a path}}(u_{ij},v_{ij},w_i,1,0). \quad (18)$$

This is similar to the first passage problem [17] when all bond weights are set to be equal. We are able to extract exact solutions in the case of homogeneous deposition rates (i.e., $\kappa_i = 1/L$ for all sites i).

IV. EXACT SOLUTIONS AND CRITICAL EXPONENTS

We consider the homogeneous case only. Then $u_{ij} \equiv u = 1/2$, $v_{ij} \equiv v = 1/2$, $w_i \equiv w = 2$, and $Q_{ij} = Q_{ji}$.

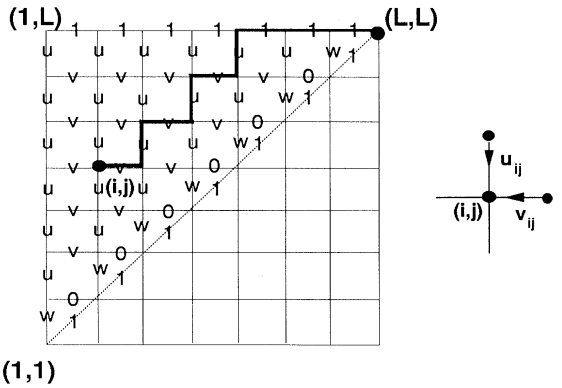

FIG. 3. Recurrence relations are mapped to a directed random walk problem in the upper diagonal half of an $L\times L$ square lattice. The thick line represents a typical path along which a directed walker can start from (L,L) and end at (i,j).

For convenience, we define normalized two-point correlation functions $\tilde{Q}_{ij} \equiv Q_{ij}/Q_{LL}$ where $Q_{LL} = 1/L$. From Eq. (18), $\tilde{Q}_{ij}$ is the sum of path weights over all possible directed paths from (L, L) to (i, j) which do not go through the lower diagonal half of the $L \times L$ square lattice. Some of these paths have the same path weights but some do not. So it is necessary to distinguish the paths with different path weights.

First, consider the case $i < j$ $(j \leq L-1)$. Paths going through a bond connecting the points (ℓ, L) and $(\ell, L-1)$ $(\ell \geq i)$ must have the same path weights,

$$\mathcal{W}(i, j; \ell) = 1^{L-\ell} u^{L-j} v^{\ell-i} = \left(\frac{1}{2}\right)^{L+\ell-i-j}. \tag{19}$$

The number of such paths, $\mathcal{N}(i, j; \ell)$, is equivalent to the number of directed paths from $(\ell, L-1)$ and to (i, j) which do not touch the diagonal line. Paths touching the diagonal line do not contribute to $\tilde{Q}_{ij}$ for $i < j$. Using the reflection principle [17], the number of paths can be easily obtained as

$$\mathcal{N}(i, j; \ell) = \binom{\ell - i + L - 1 - j}{L - 1 - j} - \binom{\ell - i + L - 1 - j}{L - 1 - i}, \tag{20}$$

where $(\cdots)$ is a combinatorial factor. Introducing new site variables for convenience $(p \equiv L-i-1,\ q \equiv L-j-1,\ r \equiv L-\ell-1)$, the normalized correlation functions are

$$\begin{aligned}\tilde{Q}_{ij} &= \sum_{\ell=i}^{L-2} \mathcal{W}(i, j; \ell)\mathcal{N}(i, j; \ell) \\ &= \frac{1}{2}\sum_{r=1}^{p} \binom{p+q-r}{q} \left(\frac{1}{2}\right)^{p+q-r} \\ &\quad - \frac{1}{2}\sum_{r=1}^{q} \binom{p+q-r}{p} \left(\frac{1}{2}\right)^{p+q-r}.\end{aligned} \tag{21}$$

This equation can be rewritten as

$$\tilde{Q}_{ij} = \frac{1}{2}\left[\sum_{m=1-k}^{q} Z_{2q}(m) - \sum_{m=1+k}^{p} Z_{2p}(m)\right], \tag{22}$$

where $k \equiv p - q = j - i > 0$, and

$$Z_{2n}(m) = \binom{2n-m}{n} \left(\frac{1}{2}\right)^{2n-m}, \tag{23}$$

which can be interpreted as the probability that a random walker in one dimension returns to the starting point exactly m times up to $2n$ steps [17]. Using identities [Eqs. (A1) and (A2) in the Appendix], Eq. (22) simplifies to

$$\tilde{Q}_{ij} = \sum_{m=0}^{k-1} Z_{2p}(m) = 1 - \sum_{m=k}^{p} Z_{2p}(m). \tag{24}$$

The diagonal elements $\tilde{Q}_{ii}$ can be written, using Eq. (15), as

$$\begin{aligned}\tilde{Q}_{ii} &= 1 + 2\sum_{j=i}^{L-1} \tilde{Q}_{j,j+1} \\ &= 1 + 2(p+1)Z_{2(p+1)}(0),\end{aligned} \tag{25}$$

where Eq. (24) and the identity of Eq. (A3) are utilized to derive the second equality. Equations (24) and (25) form a complete set of exact solutions for mass-mass correlation functions in the steady state.

Now we are ready to calculate the fluctuation properties of the surface in the RBD model. The surface height at site i, $h_i(t)$, can be written in terms of step-height variables $n_j(t)$ as

$$h_i(t) \equiv \sum_{j=1}^{i-1} n_j(t), \tag{26}$$

where $i = 2, \ldots, L$ and the reference height $h_1(t)$ is set to be zero. We consider two important fluctuations of the surface; the step-height (mass) fluctuations and the height fluctuations.

$$\begin{aligned}M_i^2(L, t) &\equiv \langle n_i^2 \rangle_t - \langle n_i \rangle_t^2, \\ W_i^2(L, t) &\equiv \langle h_{i+1}^2 \rangle_t - \langle h_{i+1} \rangle_t^2 \\ &= \sum_{j,j'=1}^{i} \left[\langle n_j n_{j'} \rangle_t - \langle n_j \rangle_t \langle n_{j'} \rangle_t\right].\end{aligned} \tag{27}$$

Notice that the fluctuations are site dependent due to the lack of translational symmetry of our RBD model. So it is useful to consider the fluctuations averaged over all sites. The average mass fluctuation in the steady state is

$$M^2(L, \infty) = \frac{1}{L-1}\sum_{i=1}^{L-1} M_i^2 = \frac{8}{3} L Z_{2L}(0), \tag{28}$$

where Eq. (25) and the identity of Eq. (A4) are used for the second equality. For large L, M^2 grows like $L^{2\alpha'}$ with exponent $\alpha' = 1/4$. It is a little tricky to calculate the average height fluctuation W^2 in the steady state. However, using a few identities of Eqs. (A4)–(A7) and Eqs. (24) and (25), we find that it is simply related to the average mass fluctuation as

$$W^2(L, \infty) = 2L - M^2(L, \infty). \tag{29}$$

For large L, W^2 grows like $L^{2\alpha}$ with exponent $\alpha = 1/2$.

The time dependence of the fluctuations, M^2 and W^2, can be investigated numerically, using the time-dependent recurrence relations in Eq. (12). We take a surface with unit step heights at every possible step $[n_i(0) = 1$ for all $i]$ as an initial configuration which is equivalent to the ensemble-averaged surface configuration in the steady-state limit $(\langle n_i \rangle_\infty = 1)$. If some other surface configurations, like a flat surface, are taken as an initial configuration, the dynamics of the growing surface involves two different time scales; one time scale associated with the evolution of the ensemble-averaged surface into the steady-state configuration and the other

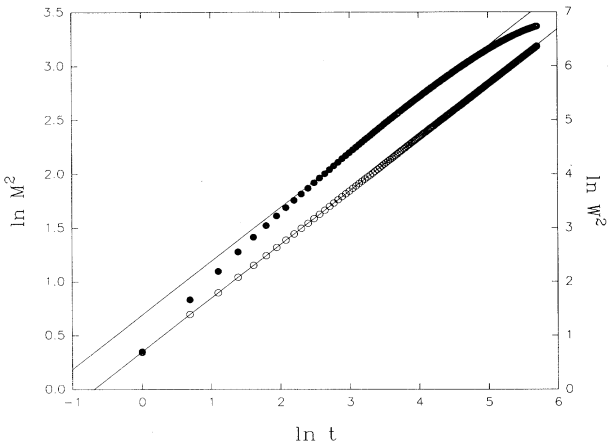

FIG. 4. Log-log plots of the average mass fluctuation M^2 (•) and the average height fluctuation W^2 (○) as functions of time t. These data are obtained by solving the recurrence relations, Eq. (12). The slopes of the lines are $2\beta' = 0.50$ and $2\beta = 1.00$.

time scale associated with the development of surface fluctuations. The former time scale is trivial and uninteresting. Moreover, the scaling exponent β in Eq. (1) characterizes the surface fluctuation time scale. We can single out the surface fluctuation time scale by choosing the above initial configuration. Starting with $\langle n_i \rangle_0 = 1$ and $\langle n_i n_j \rangle_0 = 1$, we solve the time-dependent recurrence relations, Eq. (12), iteratively. In this paper, we consider the homogeneous case only; $\kappa_i = 1/L$. The results for the average mass fluctuation M^2 and the average height fluctuation W^2 versus time t are plotted in Fig. 4 (log-log scale) for system size $L = 400$. We find that $M^2 \sim t^{2\beta'}$ with $\beta' = 0.253(5) \simeq 1/4$ and $W^2 \sim t^{2\beta}$ with $\beta = 0.500(1) \simeq 1/2$. In both cases, the dynamic scaling exponents, $z = \alpha/\beta$ and $z' = \alpha'/\beta'$, are found to be 1 ($z = z' = 1$).

V. TIME SCALES IN THE RBD MODEL AND THE SINGLE-STEP MODEL

The RBD model can be viewed as a simple variant of the single-step model by rotating the surface by 45°. As discussed in Sec. II, the RBD model with smooth particles instead of sticky particles is equivalent to the single-step model except for the boundary conditions. Depositions occur only at the valleys of the 45°-rotated surface. With *smooth* particles (or in the single-step model), the height of the valley increases by one unit at the deposition of a particle. However, with sticky particles in the RBD model, the heights of all sites between the valley and the hill increase by one unit (see Fig. 2). On average, the deposition of a particle in the RBD model is equivalent to the depositions of many particles between the valley and the hill in the single-step model. We argue that the number of depositions in the single-step model corresponding to a single deposition in the RBD model is proportional to the average surface fluctuation width W. In order to get the same morphology of the surface on average, one should wait for a much longer time t_s in the single-step model than in the RBD model. The elapsed time t_s in the single-step model is related to the elapsed time t in the RBD model as

$$t_s \sim Wt. \tag{30}$$

The surface fluctuation width of the single-step model W_s at time t_s is equivalent to that of the RBD model at time t in the infinite-size limit:

$$W(\infty, t) = W_s(\infty, t_s). \tag{31}$$

The single-step model belongs to the KPZ universality class with scaling exponents $\alpha_{KPZ} = 1/2$ and $\beta_{KPZ} = 1/3$. Using $W_s(\infty, t_s) \sim t_s^{\beta_{KPZ}}$, Eq. (31) becomes

$$W(\infty, t) \sim (Wt)^{\beta_{KPZ}}; \tag{32}$$

therefore

$$W(\infty, t) \sim t^{\beta}, \tag{33}$$

with

$$\beta = \frac{\beta_{KPZ}}{1 - \beta_{KPZ}} = \frac{1}{2}. \tag{34}$$

It is shown that the scaling exponent β is 1/2 for the RBD model by simply comparing the deposition time scales in the RBD model and the single-step model, which is consistent with our result in the previous section. It implies that these two models exhibit essentially the same scaling behavior if the time-scale difference is taken into account. Therefore the precise measurement of the exponent β in the RBD model (which is done in Sec. IV) provides the good estimate for the scaling exponents of stochastic models in the KPZ universality class.

We perform Monte Carlo simulations to confirm our argument about the time-scale difference. We take the initial configuration as a surface with $n_i(0) = 1$ for all i with horizontal length $L = 500$. After one deposition attempt on the average per lattice site (one Monte Carlo step), the time is incremented by one unit in the time scale of the RBD model. In order to use the time scale of the single-step model t_s, the time increment for an actual deposition at site i must be multiplied by the step height $n_i(t_s)$. In this time scale, we run simulations until $t_s = 5000$ and the number of independent runs is 3000. The double-logarithmic plot (Fig. 5) for the surface fluctuation width W versus time t_s shows a straight line with the slope $\beta_s = 0.338(6)$, which agrees with the KPZ value 1/3. This result confirms our previous argument about the time-scale difference between the RBD model and the single-step model. Moreover, the mass fluctuation M in this time scale also shows scaling behavior with exponent $\beta_s' = 0.168(4) \simeq 1/6$. In both cases, the dynamic exponents z_s and z_s' take the KPZ value 3/2. This result strongly supports our suggestion that the RBD model exhibits essentially the same scaling behavior as the models in the KPZ universality class if the proper time scale is employed.

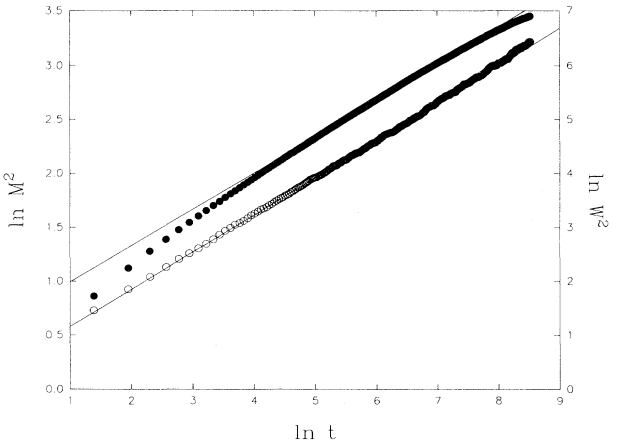

FIG. 5. Log-log plots of the average mass fluctuation M^2 (•) and the average height fluctuation W^2 (○) as functions of time t_s. These data are obtained by Monte Carlo simulations using the time scale of the single-step model. The slopes of the best-fitted lines are $2\beta' = 0.336$ and $2\beta = 0.676$.

VI. SUMMARY AND CONCLUSION

We have studied a restricted ballistic deposition (RBD) model on a one-dimensional staircase with free boundary conditions. Using the generating function method, the exact solutions for the surface fluctuation and the mass fluctuation were obtained for any system size in the steady-state limit. The RBD model is one of a few nontrivial stochastic models which can be solved exactly. We also examined time-dependent solutions by solving the recurrence relations of two-point correlation functions numerically. From these solutions, we extracted the values of the scaling exponents α and β, both of which turned out to be 1/2.

The RBD model is quite different from the ordinary ballistic deposition (BD) model because the RBD model does not allow down steps. Indeed, the scaling behavior of the RBD model differs from that of the BD model, which belongs to the KPZ universality class where $\alpha_{KPZ} = 1/2$ and $\beta_{KPZ} = 1/3$. However, the RBD model can be viewed as a simple variant of the single-step model which also belongs to the KPZ universality class. These two models exhibit a very similar surface morphology, and their dynamical processes are not much different on average except for the difference between deposition time scales.

We suggested that the major difference in the scaling behavior of the RBD model and the single-step model may disappear if the time-scale difference is properly taken into account. So the static exponent α should be equivalent in both models but the dynamic exponent β may be different. We explored the relation between the two exponents as $\beta = \beta_{KPZ}/(1-\beta_{KPZ})$, which is consistent with our results. Monte Carlo simulations confirm our argument about the time-scale difference.

The generalization of the RBD model into higher dimensions may be quite interesting, partly because it may serve as a useful alternative model for the indirect investigation of the KPZ universality class in higher dimensions. Also, our generating function approach allows us to investigate models with inhomogeneous deposition rates. The effect of the inhomogeneity on the surface morphology and the scaling behavior in the RBD model is currently under study.

ACKNOWLEDGMENTS

We wish to thank S. Redner for bringing this problem to our attention. This work is supported in part by the BSRI, Ministry of Education (Grant No. 94-2409), by the Korean Science and Engineering Foundation (Grant No. 931-0200-019-2), and by an Inha University research grant (1994).

APPENDIX

Some useful identities are listed in this appendix.

$$\sum_{m=0}^{n} Z_{2n}(m) = 1, \tag{A1}$$

$$\sum_{m=0}^{k-1} Z_{2n}(m) = \sum_{m=0}^{k-1} Z_{2(n-k)}(-m-1), \tag{A2}$$

$$\sum_{n=0}^{p-1} Z_{2n}(0) = 2pZ_{2p}(0), \tag{A3}$$

$$\sum_{n=0}^{p-1} nZ_{2n}(0) = \frac{2}{3}p(p-1)Z_{2p}(0), \tag{A4}$$

$$\sum_{n=0}^{p-1} n^2 Z_{2n}(0) = \frac{2}{15}p(p-1)(3p-1)Z_{2p}(0), \tag{A5}$$

$$\sum_{m=0}^{n} mZ_{2n}(m) = (2n+1)Z_{2n}(0) - 1, \tag{A6}$$

$$\sum_{m=0}^{n} m^2 Z_{2n}(m) = -3(2n+1)Z_{2n}(0) + (2n+3). \tag{A7}$$

[1] *Kinetics of Aggregation and Gelation*, edited by F. Family and D. P. Landau (North-Holland, Amsterdam, 1984); *On Growth and Forms: Fractal and Non-Fractal Patterns in Physics*, edited by H. E. Stanley and N. Ostrowsky (Martinus Nijhoff, Boston, 1986); J. Krug and H. Spohn, in *Solids Far from Equilibrium*, edited by C. Godrèche (Cambridge University Press, Cambridge, England, 1990).

[2] *Dynamics of Fractal Surfaces*, edited by F. Family and T. Vicsek (World Scientific, Singapore, 1991).
[3] B. B. Mandelbrot, *The Fractal Geometry of Nature*, (Freeman, San Francisco, 1982); T. Vicsek, *Fractal Growth Phenomena* (World Scientific, Singapore, 1989).
[4] F. Family, in *Universalities in Condensed Matter Physics*, edited by R. Jullien, L. Peliti, R. Rammal, and N. Boccara (Springer, Berlin, 1988).
[5] P. Meakin, P. Ramanlal, L. M. Sander, and R. C. Ball, Phys. Rev. A **34**, 5091 (1986).
[6] F. Family, J. Phys. A **19**, L441 (1986).
[7] S. F. Edwards and D. R. Wilkinson, Proc. R. Soc. London Ser. A **17**, 381 (1982).
[8] D. E. Wolf and J. Villain, Europhys. Lett. **13**, 389 (1990).
[9] F. Family and T. Vicsek, J. Phys. A **18**, L75 (1985).
[10] L. M. Sander, in *Solids Far from Equilibrium* (Ref. [1]).
[11] M. Plischke, Z. Rácz, and D. Liu, Phys. Rev. B **35**, 3485 (1987).
[12] J. M. Kim and J. M. Kosterlitz, Phys. Rev. Lett. **62**, 2289 (1989).
[13] M. Kardar, G. Parisi, and Y. Zhang, Phys. Rev. Lett. **56**, 889 (1986).
[14] D. Forster, D. R. Nelson, and M. J. Stephen, Phys. Rev. A **16**, 732 (1977); E. Medina, T. Hwa, M. Kardar, and Y. Zhang, *ibid.* **39**, 3053 (1989).
[15] B. Derrida, J. L. Lebowitz, E. R. Speer, and H. Spohn, Phys. Rev. Lett. **67**, 165 (1991).
[16] B. Derrida, J. L. Lebowitz, E. R. Speer, and H. Spohn, J. Phys. A **24**, 4805 (1991).
[17] W. Feller, *An Introduction to Probability Theory and Its Applications*, 3rd ed. (John Wiley & Sons, New York, 1970), Vol. I.